DRAFT

EXPERIMENTAL INVESTIGATION OF THERMAL LIMITS IN PARALLEL PLATE CONFIGURATION FOR THE ADVANCED NEUTRON SOURCE REACTOR*

M. Siman-Tov
D.K. Felde
M. Kaminaga**
G.L. Yoder

Oak Ridge National Laboratory***
P.O. Box 2009
Bldg. 9204-1, MS-8045
Oak Ridge, Tennessee 37831
(615) 574-6515

ABSTRACT

The Advanced Neutron Source Reactor (ANSR) is currently being designed to become the world's highest-flux, steady-state, thermal neutron source for scientific experiments. Highly subcooled, heavy-water coolant flows vertically upward at a very high velocity of 25 m/s through parallel aluminum fuel-plates. The core has average and peak heat fluxes of 5.9 and 12 MW/m^2, respectively. In this configuration, both flow excursion

---

**On assignment from Japan Atomic Energy Research Institute.

***Managed by Martin Marietta Energy Systems, Inc., under contract No. DE-AC05-84OR21400 with the U.S. Department of Energy.

(FE) and true critical heat flux (CHF), represent potential thermal limitations. The availability of experimental data for both FE and true CHF at the conditions applicable to the ANSR is very limited. A Thermal Hydraulic Test Loop (THTL) facility was designed and built to simulate a full-length coolant subchannel of the core, allowing experimental determination of both thermal limits under the expected ANSR T/H conditions.

A series of FE tests with water flowing vertically upward was completed over a nominal heat flux range of 6 to 14 MW/m^2 and a corresponding velocity range of 8 to 21 m/s. Both the exit pressure (1.7 MPa) and inlet temperature (45°C) were maintained constant for these tests, while the loop was operated in a "stiff" (constant flow) mode. Limited experiments were also conducted at 12 MW/m^2 using a "soft" mode (near constant pressure-drop) for actual FE burnout tests and using a "stiff" mode for true CHF tests, to compare with the original FE experiments.

To the authors knowledge, no other FE data have been reported in the literature that covers the range and combination of conditions reported in this paper. The experiments are currently proceeding to higher fluxes and velocities and many additional experiments are planned to satisfy the project requirements.

NOMENCLATURE

A	cross section area [m^2]
C	a constant [Eq. 5]
C_p	mean coolant specific heat [kJ/kgK]
E	electric voltage to test section [kV]
I	electric current to test section [A]
k	thermal conductivity [kW/mK]
L	heated length [m]
P	pressure [Pa]
Q	heat rate [kW]
$Q"$	heat flux [kW/m^2]
T	temperature [K]
th	thickness [m]
V	coolant velocity [m/s]
n	exponential constant [Eq. 5]
ΔP	pressure drop [Pa]
ρ	coolant density [kg/m^3]

Subscripts

al	aluminum
av	average across and along the test section

b	bulk coolant
c	value at the minimum ΔP point
cool	coolant
cs	cross section of the flow
fe	at flow excursion point
ex	exit
ext	external
in	inside
loc	local
loss	losses from test section
ox	oxide film layer
s	saturated
tot	total
ts	test section
w	wall

INTRODUCTION

The Advanced Neutron Source (ANS) is a state-of-the-art research reactor facility to be built at the Oak Ridge National Laboratory (ORNL) and is designed to become the world's most advanced thermal neutron flux source for scientific experiments. The core of the ANS reactor (ANSR) must therefore be designed to accommodate very high power densities using a very high coolant mass flux and subcooling level. A statistical/probabilistic approach to uncertainty analysis is being pursued in order to determine the optimal design power and simultaneously to provide the necessary safety

margin. This requires the selection of the most appropriate thermal-hydraulic (T/H) correlations and the development of uncertainty distribution profiles based on the best data available. The correlations currently used in the ANSR T/H analysis and the process of correlation evaluation and selection are discussed by Siman-Tov, et al. (1991).

The ANSR is both cooled and moderated by heavy water, and uses highly enriched uranium silicide fuel. The core is composed of two concentric annular core halves, each shifted axially and radially with respect to the other. Figure 1 shows the core configuration and the fuel plate arrangement. There are 684 parallel aluminum clad fuel plates (252 comprise the inner-lower core and 432 comprise the outer-upper core), each 1.27 mm thick, arranged in an involute geometry which effectively creates an array of thin rectangular flow channels. The coolant channels have a 1.27 mm gap width, spans of 87 mm (lower core) and 70 mm (upper core), and a 507 mm heated length. Each fuel plate has 10 mm unheated leading and trailing edges with all the channels having common inlet and outlet plenums with common nominal pressures of 3.2 and 1.7 MPa, respectively. The coolant flows vertically upward at an inlet velocity of 25 m/s and Reynolds number of 9.9×10^4. The inlet and average outlet temperatures are 45°C and 85°C, respectively. The average heat flux is 5.9 MW/m^2 with a radial and axial maximum of 12 MW/m^2.

The ANSR T/H operating conditions can be classified as having high subcooling, high flow (almost double the coolant velocity of other similar reactors), very high heat flux (compared to other reactors, research or commercial), a narrow channel gap, a very high length to diameter ratio (compared to most available data), and moderate pressure. When approaching thermal limits the flow remains highly subcooled and moderately turbulent. The fuel plate surface roughness is expected to be approximately 0.5 μm which was considered to be "hydraulically smooth" by preliminary comparison to the boundary layer thickness. The ANSR core configuration with multi-parallel-channels is subject to a potential excursive instability, called flow excursion (FE), and is

distinguished from a true critical heat flux (CHF) which would occur at a fixed channel flow rate as discussed later. The currently available correlations and experimental databases for both FE and CHF rarely cover the specific combination of ANSR operating parameters. This conclusion is reflected in Boyd's excellent survey on subcooled flow boiling CHF (Boyd, 1985) and for FE in Duffey & Hughes (1991), Lee, Dorra & Bankoff (1992), and Rogers & Li (1992). In addition, many investigators in the past did not distinguish between FE and true CHF, adding to the inconsistencies in the available FE and CHF databases, since both are very complex but different phenomena.

A Thermal Hydraulic Test Loop (THTL) was designed and built to provide known T/H conditions to a simulated full-length coolant subchannel of the ANS reactor core, allowing experimental determination of both FE and CHF thermal limits under the expected ANSR T/H conditions. Determination of these two thermal limits and the relationship between them (i.e., which one is limiting and by what margin) for the ANSR T/H conditions is the main objective of the THTL facility. However, the facility is also designed to examine other T/H phenomena, including onset of incipient boiling, single-phase heat transfer coefficients and friction factors, and two-phase heat transfer and pressure drop characteristics. Although the facility is aimed primarily for developing the T/H correlations at the ANSR nominal conditions for both normal operation and safety margin analysis, tests will also be conducted which are representative of decay heat levels at both high pressure (e.g., loss of offsite power) and low pressure (e.g., loss of coolant accident) as well as other quasi-equilibrium conditions encountered during transient scenarios. This paper will report and discuss the initial experiments performed which focused on the FE phenomena at the ANS nominal conditions with a few true CHF experiments for comparison.

EXCURSIVE FLOW INSTABILITY AND TRUE CHF (or DNB)

The cooling channels in the ANSR fuel assembly are all parallel to each other and share common inlet and outlet plenums, effectively imposing a common pressure drop across all the channels. This core configuration is subject to FE and/or flow instability (Leddineg, 1938 and 1949) which may occur once boiling is initiated in any one of the channels. The flow excursion phenomenon constitutes a different thermal limit than a true CHF or departure from nucleate boiling (DNB). In such a system, initiation of boiling in one of the channels (hot channel) can result in flow redistribution to the other, cooler channels. This process can very rapidly lead to flow starvation which then leads to a DNB in the "hot channel" at flows lower than the nominal flow rate. This is in contrast to a primary DNB which occurs at a nominally constant flow rate, referred to here as a "true CHF".

The more complete way to predict the occurrence of FE is to perform flow vs pressure drop analysis of the parallel channels involved and predict the flow redistribution that occurs as a result of the changing flow resistance in the "hot channel" under constant and common pressure drop boundary conditions. This process is quite complex and uncertain because of the uncertainties involved in predicting void fractions and pressure drops in two phase flow. In reality, after boiling starts, the flow resistance of the channel increases drastically leading to flow reduction in the channel which in turn promotes more boiling, rapidly leading to FE. It is normally accepted therefore that FE, also referred to as the onset of flow instability (OFI), will most probably occur near the point where sustained net vapor first appears, called "onset of net vapor generation" (ONVG) point (Costa, 1967) or the point of onset of significant void (OSV).

Maulbetsch and Griffith (1965), and other investigators, demonstrated analytically and experimentally the conditions under which excursive instability will occur. They have determined that

such instability will occur "if the slope of the (demand) pressure-drop vs. flow rate is more negative than that of the external supply system," or analytically:

$$\frac{d(\Delta P_{ext})}{dV} > \frac{d(\Delta P_{ts})}{dV} \qquad (1)$$

Figure 2 presents a typical plot of the pressure drop vs. flow rate relationship under various boundary conditions involved. In the case of many parallel channels between large common headers, as is the case in the ANSR, the slope of the "external supply system" is practically zero and is represented in Fig. 2 by horizontal lines (A & B). Maulbetsch and Griffith (1965) have also demonstrated this experimentally. Based on this determination, the approach used to achieve FE or OFI conditions in most of the THTL FE experiments was the detection of the test section pressure-drop minimum as the flow to the test section was reduced under a constant heat flux. This allowed repetition of many FE tests without experiencing an actual FE which normally leads to a test section failure. For confirmation and comparison, limited experiments were performed with an actual FE burnout and some with true CHF burnout where the flow was maintained constant. To accommodate these experiments, the design of the THTL system had to respond to three separate modes of operation:

(1) To perform actual FE tests with actual burnout (which normally leads to a destruction of the test section), a "soft" system was used. In this mode, a large bypass around the test section is fully open such that flow can split between the test section and the bypass to maintain an almost constant common pressure drop across both, simulating as closely as possible the ANSR configuration.

(2) To perform true CHF tests with actual burnout at constant and known flow rate, a "stiff" system was used. In this mode, the bypass around the test section is completely closed to maintain a constant flow through the test section. In addition, a near positive-displacement pump was used in the primary loop that provides a nearly constant flow rate, insensitive to the system pressure drop characteristics. Small diameter piping (to reduce volume) and a throttling valve were also used upstream of the test section inlet to enhance flow stability.

(3) To perform simulated FE tests without experiencing actual FE, a modified "stiff" system was used. In this mode, a closed or minimal bypass configuration along with a significant pressure drop across the flow control valve upstream of the test section was used to prevent actual FE or other flow instability. In this case, the potential for FE was determined by detecting the minimum pressure drop in a plot of pressure drop vs. flow rate (which coincides with the "ONVG" point), as demonstrated by Maulbetsch and Griffith (1965), Whittle and Forgan (1967), Costa (1967), Johnston (1988), Dougherty (1990), and others. Most of the FE tests were done using that approach.

Since the ANSR has many channels in parallel, an ideal bypass simulation in the THTL would require a very large bypass flow ratio ("infinite bypass") and therefore an unrealistically large pump. In practice, however, a reasonable but not ideal flow ratio can provide a very close simulation with no significant error. The lowest bypass flow ratio necessary, which still provides sufficiently constant pressure drop boundary conditions was investigated in two independent studies, one transient and one steady-state. Both studies are based on models simulating the THTL as a pressure-drop vs. flow network to determine the sensitivity of the bypass pressure-drop to changes in test section flow for a variety of bypass-to-test section flow ratios. The first model showed that bypass ratios of four and higher begin to approach the response of an "infinite bypass", with absolute flow rates within 3% of

the "infinite bypass" steady state flow rates (Felde, Yoder, and Skrzycke, 1992). The second model showed in a preliminary way that the slope of the bypass pressure-drop with the test section flow rate (supply side $d(\Delta P_{en})/dV$ in Eq. 1) exceeds the slope of the test section pressure-drop (demand side $d(\Delta P_{ts})/dV$ in Eq. 1) for a bypass ratio of 3 and higher, satisfying the condition for instability (Eq. 1). This supply side slope becomes extremely small (practically horizontal in Fig. 2) for bypass ratios above approximately 6, simulating closely the ANSR parallel channel configuration (see Fig. 2 for the supply and demand pressure drop relationships).

Knowing which of the two types of limiting phenomena, true CHF or FE, should be used as a thermal limit for the ANSR configuration is of critical importance. In most cases, FE will precede true CHF in such a configuration (Waters, 1966). However this depends on the specific conditions involved (Boyd, 1988). It was demonstrated that FE will occur at heat fluxes much lower than the CHF (as low as half) at low pressure, low velocities and low subcooling (Maulbetsch and Griffith, 1965), but the margin between them narrows as the level of these parameters increases and at a certain point the trend may even reverse. Since ANSR normally operates at moderate pressures and very high mass flux and subcooling levels, one of the main goals of the current tests is to determine this relationship between CHF and FE at the ANSR conditions.

Another critical question for the ANSR design is the application of either FE or true CHF to local fuel plate conditions, such as "hot spots" and "hot streaks", which may occur on the fuel plate over a small, limited area due to manufacturing imperfections which cause local heat flux peaking. In addition, the effect of the "hot subchannel" (defined as an axial region of a certain width along the fuel plate which gives a maximum bulk coolant temperature rise, also referred to occasionally as "hot stripe") on these thermal limits must be addressed. Because experimental evidence indicates little mixing across the span [Costa, (1967), and Waters, (1966)], FE in a "hot subchannel" can be treated as a narrow independent "subchannel" in relation to the rest of the flow in the rectangular channel.

The heat flux and subcooling in each one of these subchannels can therefore be applied independently, just as in the parallel channel configuration. The present ANSR T/H design technique applies appropriate uncertainties to each location on the fuel plate, and checks the resulting heat flux against various limiting criteria, including FE and CHF. Since it is recognized that very localized boiling will not impact the channel pressure drop sufficiently to cause flow excursion, FE is not used as a limiting criteria when the region of the fuel plate causing the limiting conditions is below a predetermined size (Yoder, et al, 1993).

FACILITY DESCRIPTION

The THTL was designed and built to provide known T/H conditions to a simulated full-length coolant subchannel of the ANS reactor core, allowing experimental determination of the thermal limits (both FE and CHF) under expected ANS T/H conditions. An isometric view of the facility is shown in Fig. 3 and a schematic diagram of the loop and its major components and instrumentation is presented in Fig. 4. A detailed description of the test facility was given by Felde, Yoder, and Skrzycke (1992). In the design process, special consideration was given to include the proper pump, test section bypass configuration, and system valving and piping, allowing operation of the system in either a "stiff" mode for true CHF experiments (actual primary burnout) and FE experiments with no actual burnout, or in a "soft" mode for true FE experiments (with actual secondary burnout) as discussed earlier. The Moyno primary circulation pump is driven by a variable speed motor through a gear drive. This pump and motor combination is capable of providing a wide range of flow and pressure conditions with near-positive displacement characteristics, which means that the flow is not sensitive to the loop pressure drop. This is necessary to allow operation in the "stiff" mode. Using the variable speed of the motor drive provides capability for operating over most of the flow-pressure

diagram up to 2.5 × 10^{-3} m^3/s (40 gpm) flow and 4.1 MPa differential pressure across the pump at 750 rpm. In combination with the test section bypass line, a very wide range of mass flow conditions at the test section is possible. In the "stiff" mode, with a closed bypass, a near-constant test section mass flux in the range of 7 to 42 Mg/m^2s can be used (the maximum mass flux being limited by the test loop overall pressure rating). In the "soft" mode, with a bypass flow ratio of 10 to 1, a maximum mass flux of 12 Mg/m^2s at a near-constant bypass pressure drop can be used. At a 5 to 1 bypass flow ratio, this maximum increases to 23 Mg/m^2s. The approximation of the ideal bypass ratio with a practical bypass ratio is in the non-conservative direction for flow excursion data but, as discussed earlier, it is believed that from a practical point of view this is a sufficiently good approximation. Additional parametric studies will be performed to quantify this effect and if necessary an additional pump will be installed parallel to the existing one to achieve even higher test section flows and higher bypass ratios.

TEST CHANNEL DESIGN

The test section and its boundary conditions are of primary interest for determining the T/H limits. The cross-section design is similar to that used by Gambill and Bundy (1964) but modified in accordance with the ANS characteristics as shown in Fig. 5. The test section simulates a single subchannel in the ANS reactor core with a cross section that has a full prototypic length (507 mm), the same flow channel gap (1.27 mm), the same material (aluminum) with surface roughness (~6.5 μm) reasonably close to that expected in the ANSR fuel plates. The channel span was scaled down to 12.7 mm (vs. 87 and 70 mm for the upper and lower core halves in the ANSR) in order to limit total power requirements to the test section. The involute shape of the plates was not simulated in order to simplify design and operation of the experiment. It was demonstrated by others that there

is little lateral fluid mixing in such rectangular channels even under two-phase flow conditions (Costa, 1967, Waters, 1966) and that span width (or span to gap ratio) does not have a significant effect on either CHF or FE (Gambill & Bundy, 1964, Whittle & Forgan, 1967). The test section wall thickness is 2.54 mm, dictated by the necessity to match the voltage/current characteristics of the test channel with the power supplies. The reduced wall thickness at the curved ends is designed to reduce the heat flux and prevent the coolant bulk temperature from peaking on the curved ends of the channel which could lead to premature burnout. The ratio of heat flux on the curved ends to that on the flats for the design shown in Fig. 5 is 36%. Possible effects of lateral and axial heat redistribution by thermal conduction within the test section metal will be considered later and taken into account through a three-dimensional conduction model.

The test channel is instrumented on the back of the channel wall with type N thermocouples using one of two methods. In one method, 0.50 mm dia thermocouples are inserted between the test channel wall and the ceramic insulator. The junction of the thermocouple is pressed against the wall by a ceramic rod inserted through the SS pressure backing and the ceramic insulator. A threaded-screw follower applies pressure on the ceramic rod to force the thermocouple against the wall. In the other method, a spring-loaded ribbon-type thermocouple is inserted via a bayonet mount through the SS backing and ceramic insulator with the exposed ribbon pressing against the channel wall. The locations of these thermocouples on the test section are shown in Fig. 6. The spacing is staggered as shown, to provide improved definition in the region close to the channel's exit, where FE or CHF are expected. Measurements are made on both sides of the channel for the axial locations shown for redundancy. Pressure and temperature of the water are measured at the test section inlet and outlet with the pressure taps installed in the test section flanges as shown in Fig. 6. The taps are located axially 12.7 mm from the "heated" channel at each end allowing a closer determination of the pressure-drop across the heated region without the effects of possible

condensation and dynamic pressure recovery that can occur between the end of the heated channel and the point of pressure measurement (Costa, 1967).

The test channel is enclosed inside a stainless steel pressure backing and is isolated thermally and electrically from this backing by Mycalex insulation. The test channel is either welded or brazed on both ends into aluminum flanges, each 2.54 cm thick. The test section flanges are sandwiched between two 2.54 cm thick aluminum electrical bus plates. The water connection to the test section is made concentrically inside this bus connection by a 5.08 cm flange and teflon gasket which are fastened through the test section flange. The teflon gasket and micarta bolt sleeves provide electrical isolation for the piping loop. The stainless steel backing which is in direct contact with the test section flanges at both ends is split in the center and isolated at this point by Mycalex insulation. This design effectively separates the electrical contact requirements from the water sealing requirements of the loop interface.

EXPERIMENTAL PROCEDURES

Prior to installation of the test channel assembly into the loop, the channel surface undergoes a surface treatment procedure similar to that used for fuel elements in the High Flux Isotope Reactor at ORNL and expected to be used for the ANSR fuel elements. This procedure involves cleaning and degreasing followed by an acid treatment and hot water rinse. In addition, the as-fabricated flow channel gap is measured at locations along the axial length using a capacitance-type probe inserted into the channel. This data is used to provide improved conversion of volumetric flow measurements (made upstream of the test section) to local velocities in the channel.

Flow excursion tests (without burnout) are conducted in a "stiff" mode using a closed or minimal bypass flow configuration, along with a significant pressure drop across the flow control valve upstream of the test section to prevent actual excursion as discussed earlier. The test is initiated by

setting test section flow to a level where no boiling will exist at the target heat flux level. The applied power to the test section is then raised to produce the target heat flux level. Exit pressure is automatically controlled via the system letdown valve and high pressure make-up pump at the desired setting (nominally 1.7 MPa). Process water flow to the secondary side of the heat exchanger is also automatically controlled to maintain the inlet bulk coolant temperature at the desired setpoint (nominally 45°C). Data is recorded continuously during these processes by the PC-based data acquisition system. Once the system is stabilized and data obtained under steady-state conditions, the velocity is reduced to a lower level while monitoring the measured differential pressure across the test channel. This reduction is made through either pump speed reduction, flow control valve positioning, bypass flow adjustment, or some combination of the above, depending on the proximity of the conditions to the expected minimum. As the minimum is approached, the loop configuration is adjusted to minimize the amount of bypass flow and maximize the pressure drop across the control valve in order to prevent an actual excursion and channel failure. The system is allowed to stabilize at each of the velocity settings selected. Power supply adjustments are made concurrent with velocity changes in order to maintain the average heat flux constant (since the temperature coefficient of resistivity of the aluminum affects the current-voltage characteristics of the test channel as velocity is reduced and test channel wall temperatures increase). Once the minimum in pressure drop has been determined (by observation of increasing pressure drop as velocity is further decreased), the velocity is increased once again, and data is taken at some of the velocity points obtained during the earlier sequence for comparison.

DATA REDUCTION AND ANALYSIS

An experimental data reduction model was developed for single-phase forced-convection flow, focusing on the flat portion of the test channel. Fundamental variables required to identify heat transfer characteristics in single-phase forced-convection heat transfer are local heat flux Q''_{loc}, local inside surface temperature $T_{w,in}$ of test section, local bulk coolant temperature T_b and coolant velocity V in the flat channel. Local heat flux Q''_{loc} is not uniform over the test section because the resistivity of the aluminum test section depends on its temperature. Therefore local heat flux on the flats Q''_{loc} is calculated based on temperature dependent resistivity of the aluminum test section and the average heat flux on the flat Q''_{av}. The latter is determined based on the total heat input Q_{tot} into the test channel, as follows:

$$Q''_{av} = Q_{tot} \cdot (1-Q_{loss}) \cdot th_{al} / (L \cdot A_{al}) \qquad (2)$$

Total heat input Q_{tot} is given by the product of the current I and the voltage E applied to the test section. Heat loss Q_{loss} is calculated by comparing the heat input Q_{tot} with the heat rate Q_{cool} transferred to the coolant, as follows:

$$Q_{loss} = 1 - Q_{cool}/Q_{tot} = 1 - \frac{\rho V A_{cs} C_p \Delta T_b}{EI} \qquad (3)$$

The heat loss range of FE tests conducted was calculated to be between 5 to 12% of Q_{tot} with the higher values being for the lower velocities. Coolant flow velocity V in the flat channel is converted from average coolant velocity V_{av} so that the pressure-drop of the flat channel is equal to that of the curved end channels.

As already described, the temperature of the test section required to identify the heat transfer characteristics is the surface temperature $T_{w,in}$ on the flow channel side, but the thermocouples are

attached on the surface on the ceramic insulator side. Therefore $T_{w,in}$ is determined based on the local heat flux Q''_{loc} in the flats, as follows:

$$T_{w,in} = T_{w,ex} - Q''_{loc} \cdot th_{al} / 2 \cdot k_{al} - Q''_{loc} \cdot th_{ox} / k_{ox} \quad (4)$$

The experimental data reduction model also includes a single-phase pressure drop calculation model. As described earlier, the test section inlet and outlet pressures were measured at the taps installed in the test section flanges, which are located axially 12.7 mm from the "heated" channel at each end. The pressure-drop of the "heated" channel ΔP_{ts} was converted from a measured pressure-drop by excluding the pressure-drops across the "non-heated" sections. The pressure-drop across the "non-heated" section between the end of the test channel and the pressure tap is calculated with the Darcy friction factor using the Filonenko correlation (Filonenko, 1954).

RESULTS AND DISCUSSION

The THTL experimentation for the ANSR T/H correlations is still in its initial stages. The current THTL (Figs. 3 & 4) and test section design (Figs. 5 & 6) are the result of a number of initial shakedown and benchmark tests, which led to successive modifications both in the loop and the test section design. The initial emphasis was put on the FE phenomena at nominal conditions. The first goal was to proceed from low levels of heat flux and velocity then extend the tests to the extremely high levels required by the ANSR operating conditions. The experiments accomplished so far include the following T/H conditions:

Coolant: Water

Inlet coolant temperature: 45°C

Exit coolant pressure: 1.7 MPa

Nominal average heat flux range: 6 - 14 MW/m^2 (goal is 17 MW/m^2)

Corresponding velocity range: 8 - 21 m/s (goal is 27 m/s)

Channel configuration (Figs. 5 & 6): Rect., 1.27 × 12.7 × 507 mm

A non-powered data set of pressure-drop across the test section as a function of velocity was made prior to powered operation and repeated after every few runs in the test sequence. This was done to provide a reference with the expected single phase pressure-drop under isothermal conditions. It also effectively monitors any possible accumulated channel geometry changes from previous powered operation. The heat fluxes covered so far include the nominal values of 6, 9, 11, 12, 13, and 14 MW/m^2 with the resulting respective average velocities of 8.1, 12.5, 16.6, 17.3, 18.8, and 20.4 m/s, as determined at the point of minimum pressure-drop. Acquiring FE data at this level of heat fluxes and velocities is of significance for two reasons. First, to the authors knowledge, no data is available for velocities higher than 10 m/s [Duffey & Hughes (1991), Lee, Dorra & Bankoff (1992), and Rogers & Li (1992)], except those reported by Waters (1966) at 16 m/s in experiments supporting the Advanced Test Reactor. Second the heat flux achieved is beyond the ANS nominal peak heat flux of 12 MW/m^2. The corresponding limiting velocity of 17.3 m/s is much below the ANS nominal velocity of 25 m/s; even at the highest heat flux tested (14 MW/m^2 average and 16.2 MW/m^2 at the exit) the corresponding velocity of 20.4 m/s is well below the ANSR nominal operating velocities. This implies, on a preliminary basis, that there exists a good margin in the ANSR operating velocity.

It was a general practice to re-check a few of the pressure drop measurements as velocity was increased back upward along the velocity curve (following the sequence where velocity is decreased to find the minimum) and in some cases the runs were duplicated for confirmation. The differences found in velocities at the minimum pressure drop points were small and the above quoted velocities are an average of the repeated cases. However, in the high heat flux cases of 13 and 14 MW/m^2

pressure drops were higher when measurements were repeated for the same velocities. The actual data from the sequences performed for each case on decreasing velocity are summarized in Table 1 and in Figs. 7 & 8, including two of the non-powered cases. It is worth emphasizing that the heat fluxes indicated for each curve are nominal average values. The actual local heat flux close to the exit (where the FE phenomena is supposed to start) are indicated in Table 1 as Q''_{ex} which are in all cases higher due to the aluminum resistivity change with temperature. For example, the local heat flux at the exit corresponding to the 14 MW/m^2 nominal is 16.2 MW/m^2, which is the value used for comparison with correlations. As can be seen in the Fig.'s 7 & 8, the minimum points could be clearly detected and in none of the experiments was the true CHF (or the subsequent expected burnout) encountered before that minimum, which is the point where FE would occur.

A single case of true CHF was also performed at 12 MW/m^2 using the "stiff" system mode (closed bypass). The corresponding CHF velocity was 12.2 m/s as compared to the corresponding FE velocity of 17.3 m/s. This shows an additional margin in velocity of about 30% compared to the FE velocity and of about 50% margin compared to the ANSR nominal velocity.

Although the final correlation of the FE data will be postponed until the remainder of the experiments are performed (by extending the heat flux and corresponding velocity ranges up to 17 MW/m^2 and about 27 m/s, respectively) the data collected was plotted in Fig. 9 and comparisons were made with correlations by Costa (1967), Whittle & Forgan (1964), and Saha & Zuber (1974). The Costa correlation is the one currently being used for the preliminary ANSR T/H design and analysis. Whittle and Forgan (W&F) and Saha and Zuber (S&Z) correlations are widely used in the USA with the S&Z correlation being well established in many computer codes for nuclear safety analysis. For a given coolant (water), physical properties, and geometry (L/D=199.6) all three correlations can be rearranged and simplified to the same general formulation as follows:

$$Q''_{fe} / (T_s - T_b)_{fe} = C\, V^n \qquad (5)$$

where: Costa: C = 1/0 0128, n = 0.5

Saha & Zuber: C = 1/0.0382, n = 1.0

Whittle & Forgan: C = 1/0.0427, n = 1.0

In the Costa correlation, the FE heat flux is proportional to the square-root of velocity whereas both W&F and S&Z (as well as most other FE correlations) show a linear dependence. Based on this formulation, the Costa correlation will yield the same result as the W&F correlation at a velocity of 11.1 m/s and will be too optimistic (higher heat flux) at lower velocities and too conservative at higher velocities (33% more conservative than W&F at the ANSR nominal velocity of 25 m/s). The Costa correlation will show the same trend when compared with the S&Z correlation, except that the equality will occur at 8.9 m/s. At 25 m/s it will be about 40% more conservative than S&Z. Since the above correlations are based on data for relatively low velocities (maximum of 9.14, 7, and 7.66 m/s for W&F, Costa, and S&Z, respectively) it is quite interesting to see the trend of our data in terms of dependence on velocity. A comparison of the data with the three correlations is shown in Fig. 9. All three correlations seem to be conservative when compared to the data, with S&Z being in best agreement. Excluding 3 of the 4 data points taken with test section TSD-3/B (a possible anomally with this section is being investigated), the agreement with S&Z is quite good, with the correlation skirting the lower bound of the data. The FE heat flux dependence on velocity seems to be between 0.5 power (Costa) and 1.0 (S&Z and W&F), more nearly in the 0.8 to 0.9 range. This is in agreement with the conclusion recently arrived at by Lee & Bankoff (1992), and Rogers & Li (1992) who relate the heat flux to the turbulent heat transfer coefficient (which is approximately proportional to the 0.6-0.8 power of velocity). As indicated before, the actual correlation of the ANSR FE data is postponed to a later stage.

FUTURE PLANS

The initial focus of the THTL experimentation for the ANSR is the determination of thermal limits under ANS nominal conditions using water as coolant. Future plans include additional experiments to be performed with the existing facility and the basic test section design which can capture the onset of incipient boiling, single-phase heat transfer coefficients and friction factors, and two-phase heat transfer and pressure drop characteristics.

Also included are plans for non-nominal conditions including low-flow tests simulating shutdown and refueling conditions, low pressure conditions simulating Loss of Coolant Accidents (LOCA) and other selective quasi-equilibrium conditions encountered during transient scenarios, the effects of oxide build-up (typical to aluminum), the effects of material and its surface roughness, and the effects of heavy water on the thermal limits (CHF, FE, and IB).

Other experiments will require upgrading the THTL facility and new test section designs to accommodate additional requirements. This includes a full span single-sided heated channel to determine the level of lateral flow mixing in the channel and to confirm the effects (or lack of it) of channel span, a two-sided half-length heated channel to test the effects of lateral and axial heat flux distributions, and a full span single-sided heated channel to test the effects of "hot spots" and "hot streaks" on CHF and FE thermal limits, respectively.

In the near term, the current series of experiments will be continued to accomplish the following:

1. Extend the current FE sequence to achieve or exceed the ANSR nominal set point conditions, which include the nominal velocity of 25 m/s and the corresponding heat flux of about 16 MW/m^2 using the minimum pressure-drop approach (modified "stiff" system with closed or minimal bypass).

2. Confirm that indeed actual burnout FE (destructive FE) does occur at the point of minimum pressure-drop, using a "soft" system with open bypass.
3. Perform selective true CHF tests to establish the relationship between true CHF and FE, using a "stiff" system with closed bypass, focusing on the ANS nominal operating conditions.
4. Establish the correlation of FE and CHF as a function of the major T/H parameters of velocity, pressure, and subcooling at the range of the ANS nominal conditions (nominal set point plus/minus 20%).
5. Perform tests on special effects of the thermal limits (oxide film, D_2O, etc.) and on non-nominal conditions as well as on other T/H phenomena, as described earlier for the long range plans.

SUMMARY AND CONCLUSIONS

1. A THTL facility was constructed with special consideration given to assure the capability to operate the loop in three different modes, "stiff" mode for CHF tests, "soft" mode for actual flow excursion burnout tests, and "modified stiff" mode for non-destructive FE tests (minimum pressure drop) simulating the multiple parallel channel configuration of the ANSR as close as possible. This includes a bypass line in parallel to the test section, a large nearly positive-displacement pump providing nearly constant mass flux, and reduced volume piping upstream of the test section, along with a significant pressure drop across the flow control valve upstream of the test section.
2. Although the experiments performed so far are in their initial stages, preliminary conclusions were derived by comparing the data to three well-known flow excursion correlations of Costa (1967), Whittle & Forgan (1964), and Saha & Zuber (1974). All three correlations seem to be conservative when compared to the data, with Saha & Zuber showing the best agreement.

The flow excursion heat flux dependence on velocity seem to be somewhere between 0.5 power (Costa) and 1.0 (S&Z and W&F), more nearly in the 0.8 to 0.9 range, in agreement with more recent correlations by Lee & Bankoff (1992) and by Rogers & Li (1992).

3. Acquiring the flow excursion data at this level of heat flux and velocity is of great significance for a number of reasons. Most of the available flow excursion data is in the low velocity range (less than 10 m/s). The data reported in this paper is beyond any that was available to date, except those reported by Waters (1966) in support of the Advanced Test Reactor. The heat flux achieved (14 MW/m^2 average and 16.2 MW/m^2 at the exit) is well beyond the ANSR peak heat flux of 12 MW/m^2 and yet the corresponding limiting velocity is 17.3 m/s, well below the ANSR nominal velocity of 25 m/s. In none of the experiments performed so far was the true CHF (or the subsequent expected burnout) encountered before the minimum pressure drop (flow excursion) point. Furthermore, a true CHF test at 12 MW/m^2 showed a corresponding velocity of 12.2 m/s as compared to the 17.3 m/s for the FE velocity (30% margin) and 50% margin compared to the ANSR nominal velocity. This implies, on a preliminary basis, that there exists a good safety margin in the ANSR operating velocity for both thermal limits.
4. The initial focus in the THTL experimentation for the ANSR is on thermal limit determination under ANSR nominal conditions using water as the coolant. A comprehensive test plan for the THTL facility and its various upgrades is being developed, taking into account all the phenomenon and effects intended to be studied in that facility and the constraints involved. Upgrades planned for the THTL facility include a full-span, single-sided heated channel, a two-sided, half-length heated channel, and a full-span, single-sided heated channel.

corresponding heat flux of 16 MW/m^2. The final correlation of the data for FE and CHF as a function of the major T/H parameters at the ANSR conditions range is postponed until the remainder of the experiments are performed.

ACKNOWLEDGEMENT

The authors would like to acknowledge the support of the ANS Project Office that made this work possible and the support received from Marshall McFee, Bill Nelson, Art Ruggles, Ronald Boyd, and other contributors.

REFERENCES

Boyd, R. D., January 1988, "Subcooled Water Flow Boiling Experiments Under Uniform High Flux Conditions," Fusion Tech., Vol. 13, pp. 131-142.

Boyd, R. D., January 1985, "Subcooled Flow Boiling Critical Heat Flux (CHF) and Its Application to Fusion Energy Components. Part I: Fundamentals of CHF," (p. 19), and Part II: A Review of Microconvective, Experimental, and Correlational Aspects," (p. 31), Fusion Tech., 7, 1.

Costa, J., 1967, "Measurement of the Momentum Pressure Drop and Study of the Appearance of Vapor and Change in the Void Fraction in Subcooled Boiling at Low Pressure," [in French: "Measure de la perte de pression par acceleration. Etude de 1' appartition dela vapor et evolution de teaux de vide en ebullition locale a basse pression"] Communication presented at the Meeting of the European Group Double-Phase, Winfrith, 1967. Translated from French as ORNL/TR-90/21.

Duffey, R. B. and Hughes, E. D., November 1990, "Static Flow Instability Onset in Tubes, Channels, Annuli, and Rod Bundles," ASME HTD-Vol. 150, Winter Annual Meeting, Dallas, TX.

Dougherty, T., et al., December 1989, "Flow Instability in Vertical Down-Flow at High Fluxes," ASME HTD-Vol. 119, Winter Annual Meeting, San Francisco, CA.

Felde, D. K., G. L. Yoder, and D. Skrzycke, May 1992, "The Advanced Neutron Source Thermal Hydraulic Test Loop," presented at *8th Power Plant Dynamics, Control & Testing Symposium*, Knoxville, TN.

Filonenko, G. K., 1954, "Hydraulic Resistance in Pipes (in Russian)," *Teploenergetika*, Vol. 1, No. 4, pp. 40-44.

Gambill W. R., and Bundy, R. D., 1964, "Heat Transfer Studies of Water Flow in Thin Rectangular Channels, Part I: Heat Transfer, Burnout, and Friction for Water in Turbulent Forced Convection," Nucl. Science and Eng., Vol. 18, pp. 69-79.

Johnston, B. S., 1988, "Subcooled Boiling of Downward Flow in a Vertical Annulus," Report No. DPST-88-891, Savannah River Laboratory, Aiken, SC.

Leddineg, M., 1938, "Unstabitit der Stromung bei naturlichen und Zwangumlauf," *die Warme*, **61**(48), 891-898.

Leddineg, M., 1949, "Flow Distribution in Forced-Circulation Boilers," *The Engineering Digest,* **10**, 85-89.

Lee, S. C. and Bankoff, S. G., August 1992, "Prediction of the Onset of Significant Void in Down Flow Subcooled Nucleate Boiling," ASME HTD-Vol. 197, *Proc. of 28th National Heat Transfer Conference and Exhibition,* San Diego, California.

Lee, S. C., Dorra, H., Bankoff, S. G., 1992, "A Critical Review of Predictive Models for the Onset of Significant Void in Forced-Convection Subcooled Boiling," ASME HTD-Vol. 217, Winter Annual Meeting, Anaheim, CA.

Maulbetsch, J. S. and Griffith, P., April 1965, "A Study of System-Induced Instabilities in Forced-Convection Flows with Subcooled Boiling," MIT, Department of Mechanical Engineering, Report No. 5382-35.

Rogers, J. T. and Li, J., November 1992, "Prediction of the Onset of Significant Void in Flow Boiling of Water," Fundamentals of Subcooled Flow Boiling, ASME HTD-Vol. 217, Winter Annual Meeting, Anaheim, CA.

Saha, P. and N. Zuber, 1974, "Point of Net Vapor Generation and Vapor Void Fraction in Subcooled Boiling," *Proc. of 5th Int. Heat Transfer Conf.,* Tokyo, Vol. IV, pp. 175-179.

Siman-Tov, M., et al, December 1991, "Thermal-Hydraulic Correlations for the Advanced Neutron Source Reactor Fuel Element Design and Analysis," ASME HTD-Vol. 190, Winter Annual Meeting, Atlanta, GA.

Waters E. D., May 1966, "Heat Transfer Experiments for Advanced Test Reactor," BNWL-216, UC-80 (TID-4500).

Whittle, R. H. and Forgan, R., 1967, "A Correlation for the Minima in the Pressure Drop vs. Flow-Rate Curves for Sub-Cooled Water Flowing in Narrow Heated Channels," *Nuclear Eng. & Design*, Vol. 6, pp. 89-99.

Yoder, et al., 1993, "Preliminary T/H Analysis of the Advanced Neutron Source Reactor Core for the CSAR," to be published.

Table 1. Results summary of flow excursion tests in the THTL[1]

Test Case	Date	Q" MW/m²		V_c	$\Delta P_{ts,c}$	$P_{ex,c}$	$T_{b,ex}$	Q_{loss}	V_1	$\Delta P_{ts,1}$
		$Q"_{av}$	$Q"_{ex}$	m/s	MPa	MPa	°C	%	m/s	MPa
FE817A	08/17/92	No power		-	-	-	-	-	26.6	1.254
FE903A	09/03/92	No power		-	-	-	-	-	27.9	1.487
FEN17A	11/17/92	No power		-	-	-	-	-	28.1	1.514
FEN17D	11/17/92	No power		-	-	-	-	-	28.1	1.491
FEN19A	11/19/92	No power		-	-	-	-	-	28.3	1.483
FEN20C	11/20/92	No power		-	-	-	-	-	28.0	1.468
FEN30B	11/30/92	No power		-	-	-	-	-	30.0	1.643
FED15A	12/15/92	No power		-	-	-	-	-	40.2	2.771
FED17B	12/17/92	No power		-	-	-	-	-	36.1	2.244
FED28A	12/28/92	No power		-	-	-	-	-	30.0	1.619
FE817C	08/17/92	6.0	6.4	8.1	0.110	1.653	182.5	11.0	17.2	0.456
FE904A	09/04/92	6.1	6.5	8.1	0.147	1.670	190.1	9.2	18.0	0.541
FE904B	09/04/92	9.1	9.9	12.5	0.307	1.617	188.0	8.7	22.1	0.746
FEN17B	11/17/92	8.9	9.6	12.5	0.297	1.728	182.5	11.7	22.2	0.764
FE904C	09/04/92	11.3	12.4	16.6	0.456	1.571	178.3	7.7	24.1	0.853
FE904D	09/04/92	12.3	13.8	17.5	0.545	1.530	182.3	7.6	25.1	0.913
FEN17C	11/17/92	12.0	13.0	17.4	0.510	1.705	178.1	10.5	28.1	1.114
FED15B	12/15/92	12.1	13.1	17.1	0.547	1.718	181.9	9.7	28.0	1.147
FEN20A	11/20/92	13.1	14.5	19.0	0.607	1.739	178.6	10.3	30.0	1.269
FED15C	12/15/92	13.1	14.2	18.6	0.634	1.733	181.3	9.4	36.0	1.877
FEN20B	11/20/92	14.2	16.0	20.5	0.744	1.728	180.0	9.0	30.0	1.248
FEN30A	11/30/92	14.2	16.2	20.5	0.757	1.725	180.7	8.8	30.0	1.334
FED17A	12/17/92	14.0	15.6	20.5	0.750	1.701	176.8	10.1	36.0	1.906
FED28B	12/28/92	14.1	14.8	20.0	0.768	1.738	181.1	9.7	35.9	2.070

[1] In all cases: P_{ex} = 1.7 MPa, T_{in} = 45 °C.
$T_{b,ex}$ - exit bulk coolant temperature.
Q" - heat flux.
av - average nominal.
b - bulk.
ex - exit (maximum).
ts - test section.
c - value at the minimum ΔP point.
1 - value at the first data point of the case.
loss - heat losses from test section.

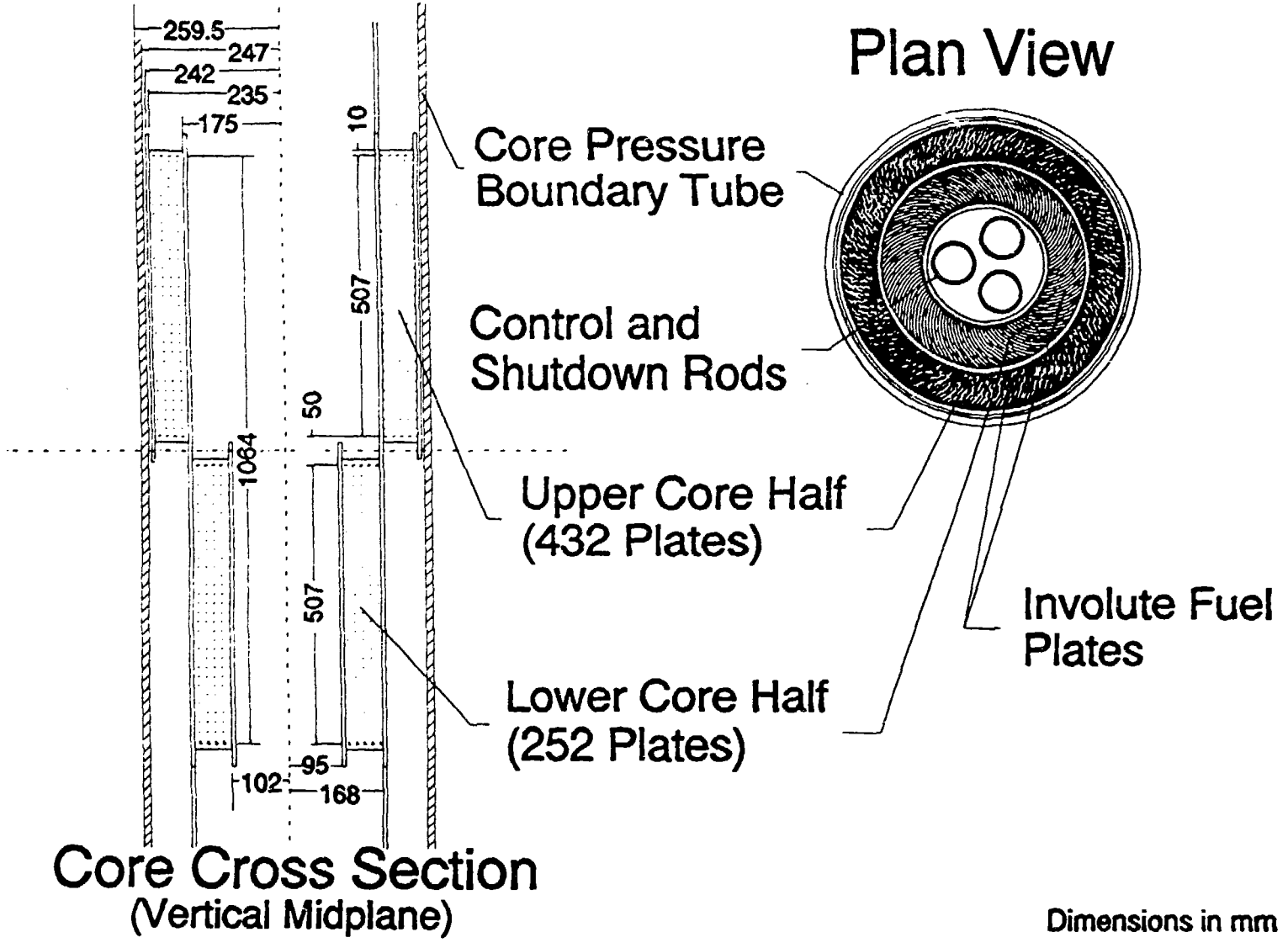

Fig. 1. ANSR core assembly and fuel plates arrangements.

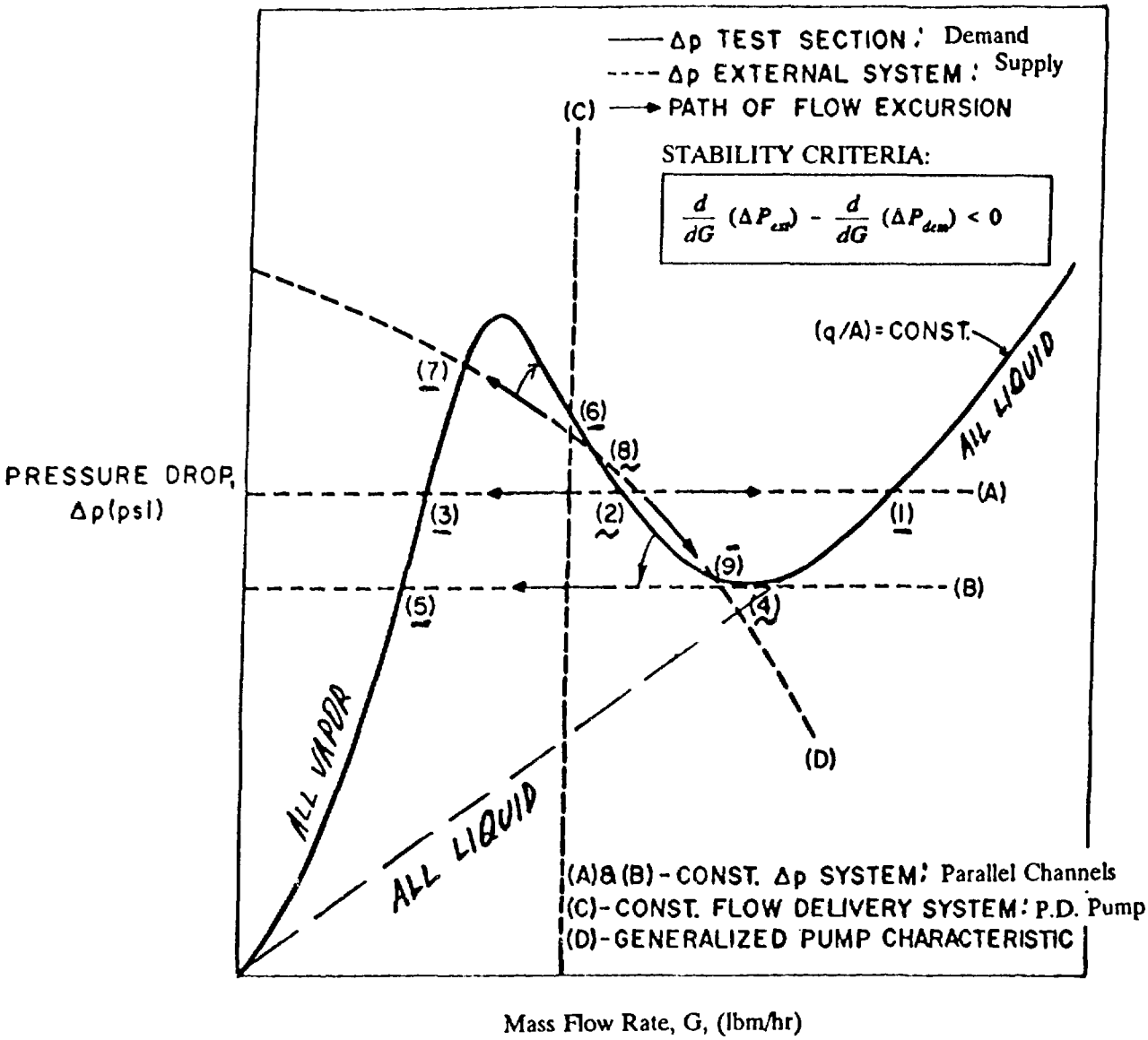

Fig. 2. Graphical interpretation of excursive instability (Fig. modified from Maulbetsch & Griffith, 1965).

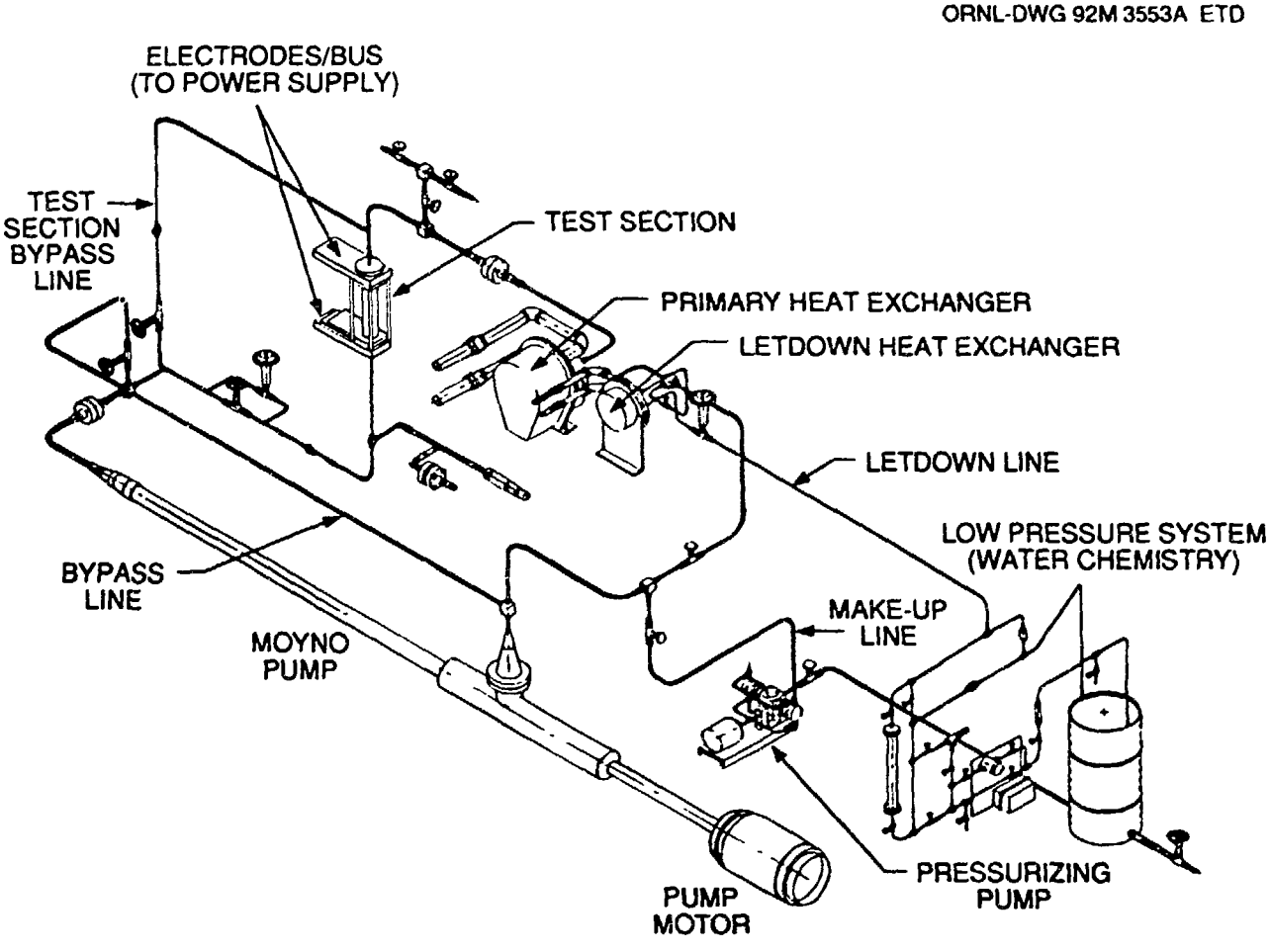

Fig. 3. Advanced Neutron Source (ANS) Thermal Hydraulic Test Loop.

Figure 4. Schematic diagram of the THTL primary components and instrumentation.

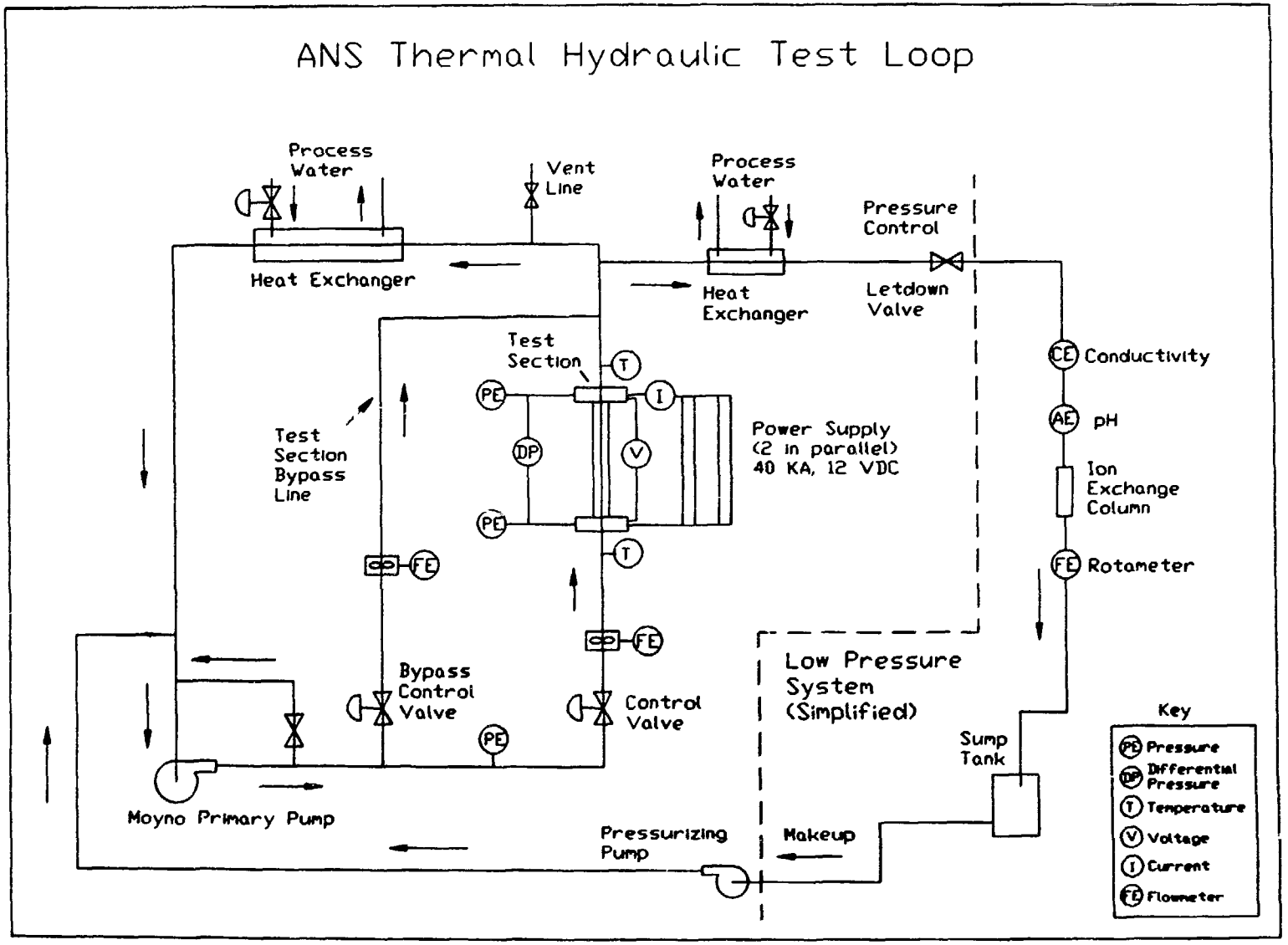

Figure 5. Cross-section of the test channel in the THTL.

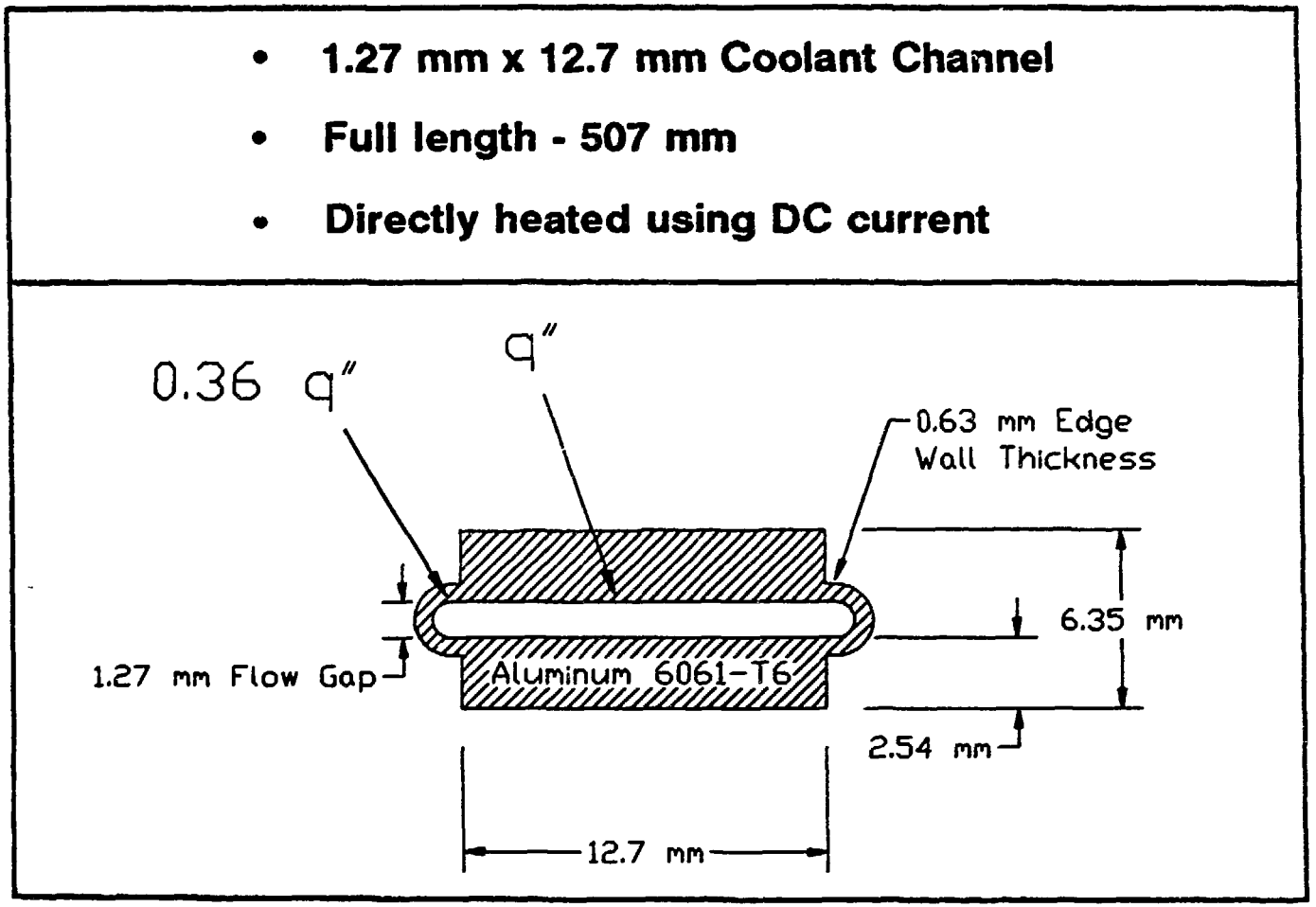

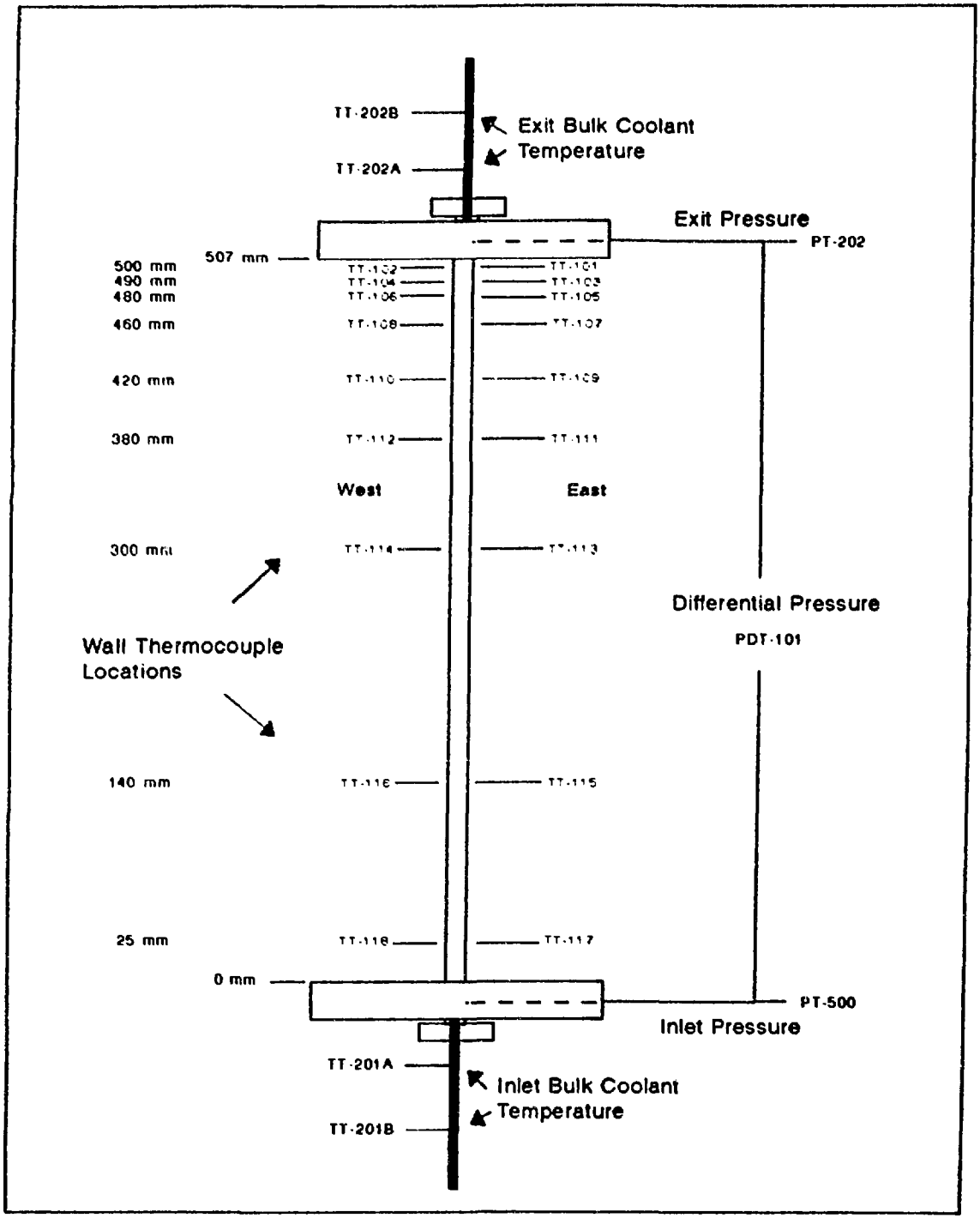

Fig. 6. THTL Test Section Instrumentation.

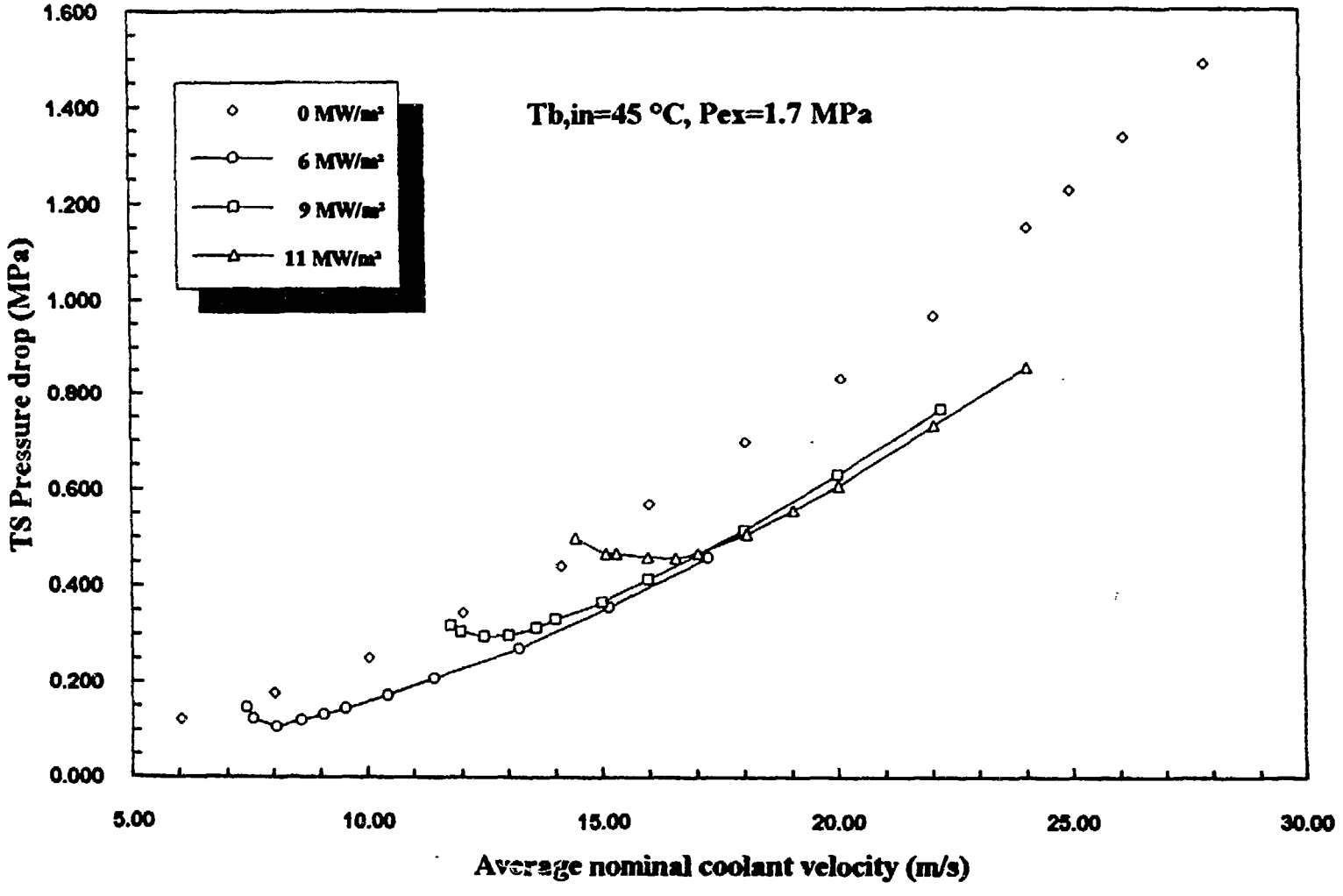

Fig.7 Flow Excursion Data from THTL Experiments

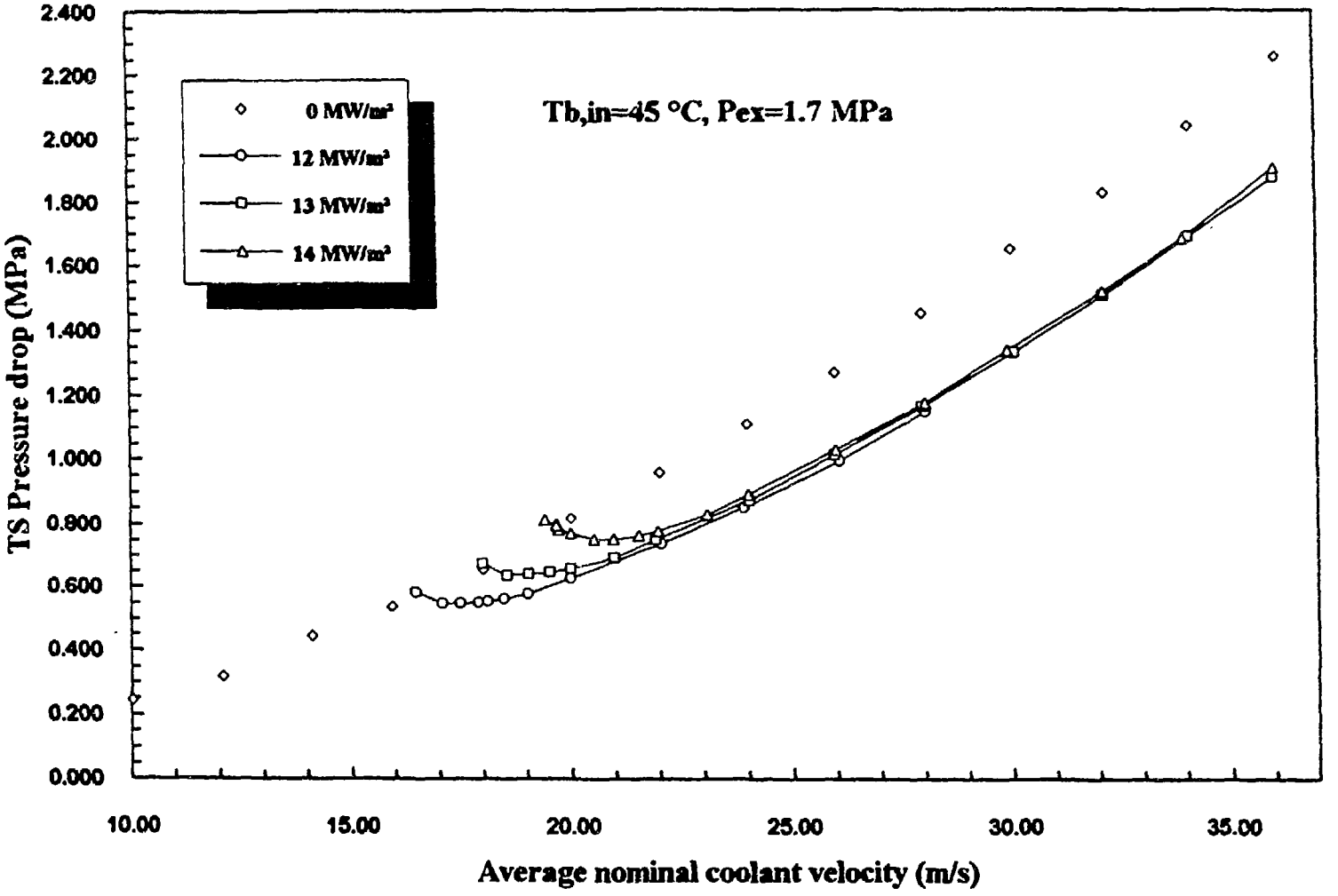

Fig.8 Flow Excursion Data from THTL Experiments

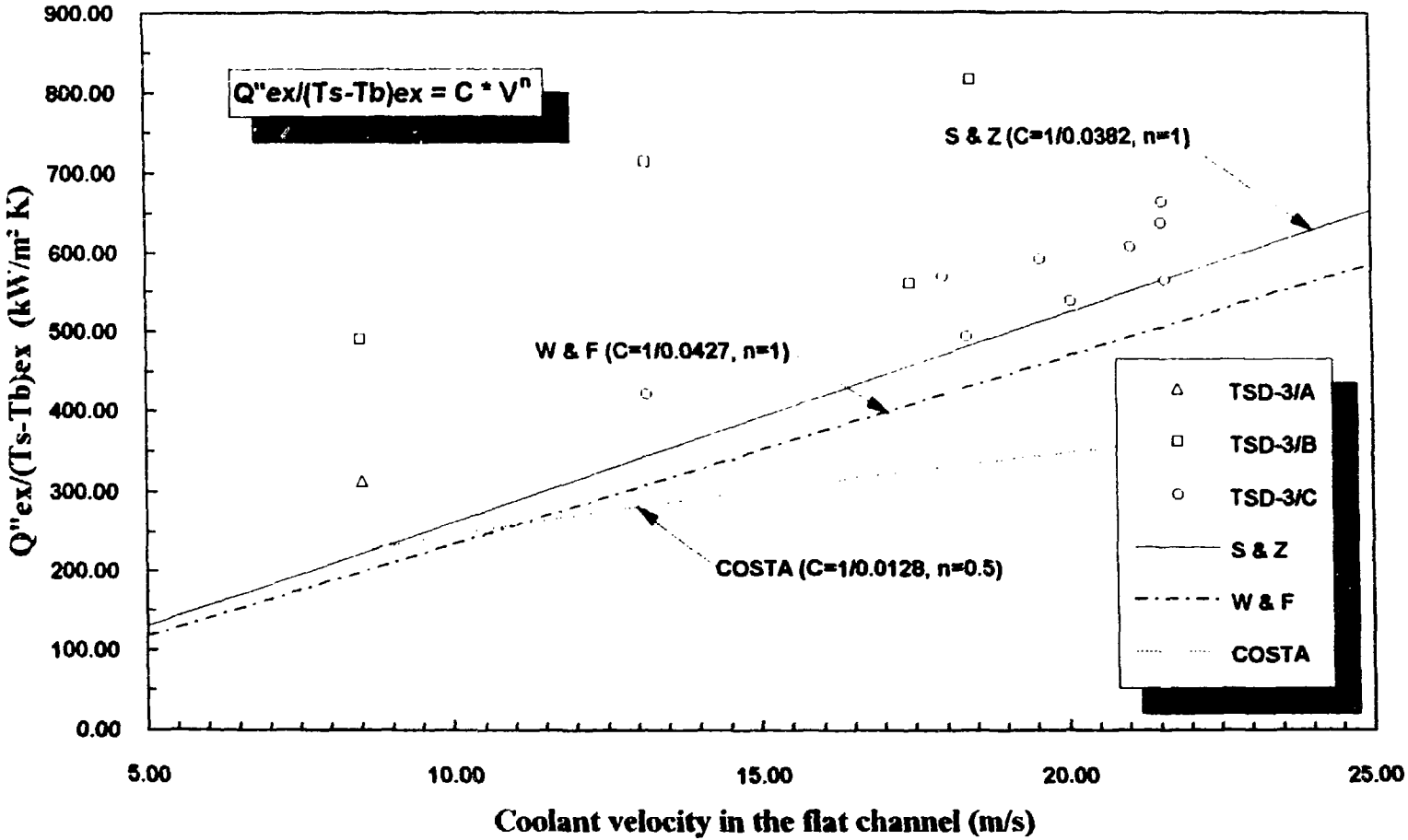

Fig. 9 Flow Excursion Data From THTL Experiments